

The Kondo effect in pseudo-gap Fermi systems: a renormalization group study

This article has been downloaded from IOPscience. Please scroll down to see the full text article.

1995 J. Phys.: Condens. Matter 7 L491

(<http://iopscience.iop.org/0953-8984/7/37/003>)

View [the table of contents for this issue](#), or go to the [journal homepage](#) for more

Download details:

IP Address: 171.66.16.151

The article was downloaded on 12/05/2010 at 22:06

Please note that [terms and conditions apply](#).

LETTER TO THE EDITOR

The Kondo effect in pseudo-gap Fermi systems: a renormalization group study

Kan Chen[†] and C Jayaprakash[‡]

[†] Department of Physics and Computational Science Programme, National University of Singapore, Singapore 0511

[‡] Department of Physics, The Ohio State University, Columbus, OH 43210, USA

Received 19 June 1995

Abstract. We present a Wilson renormalization group study of the Kondo problem in a pseudo-gap Fermi system with density of states $\rho(\epsilon - \epsilon_F) = C|\epsilon - \epsilon_F|^r$. For initial couplings $J_0 < J_c \approx -2r$ the impurity spin is quenched, but we find that the model exhibits unusual low-temperature properties unique to pseudo-gap systems. For $r < 0.5$ the ground state is characterized by the $J = -\infty$ fixed point, with a residual magnetic moment and non-vanishing entropy. The magnetic susceptibility is shown to fit the universal curve, $T\chi(T) = r/8 + (1 - r - 3r^2/2)f(\frac{1}{2}((T/T_K)^{1-2r} + (T/T_K)^{1-r}))$, where $f(x)$ is the universal function for the ordinary Kondo problem. For $r > 0.5$ we also find the quenching of the impurity spin, yet there is no Kondo effect exhibited in the total magnetic susceptibility.

Many interesting materials can be described with Fermi systems with a pseudo-gap, i.e. a gapless energy spectrum with a vanishing density of states at the Fermi level. This situation arises, for example, in bulk semiconductors and (quasi-) two-dimensional metals when the conduction and valence bands touch at the symmetry points of the Brillouin zone. Some single-particle excitations in anisotropic superconductors also exhibit pseudo-gap spectra. The interaction of magnetic ions with the electrons of such systems can lead to different properties from those in normal Fermi systems. Obviously interesting questions involve the Kondo effect, generally believed to be a phenomenon associated with the existence of a sharp Fermi surface: does the Kondo effect persist in systems with a small energy gap or a pseudo-gap? If it does, what are the universal properties in the Kondo regime? In this article we present our study of the Kondo model in pseudo-gap Fermi systems. We confine our attention to pseudo-gap Fermi systems partly because we can apply Wilson's RG method using a diagonalization scheme we have developed. The RG calculation permits us to obtain physical intuition about the low-temperature properties as well as some 'almost exact' results.

The problem of magnetic impurities in pseudo-gap Fermi systems was first investigated by Withoff and Fradkin [1], who studied the Kondo model with the density of states $\rho(\epsilon) = C|\epsilon|^r$ (with band cut-off D_0 and Fermi energy set to zero) using perturbative scaling and the $1/N$ expansion to leading order. They argued that, with $r > 0$, there is a transition as the coupling constant J is varied across the critical value $J_c \propto -rD_0$: for a weak initial coupling ($J_c < J < 0$), there is no Kondo effect, while for strong initial coupling $J < J_c$, there is a Kondo effect with the Kondo temperature vanishing at J_c as $T_K \approx |J - J_c|^{1/r}$. Thermodynamic properties were not computed and differences from the Kondo effect in normal Fermi systems were not investigated. We use Wilson's RG

method, a non-perturbative technique, calculate the magnetic susceptibility as a function of temperature and perform detailed analysis of the fixed points. While our results confirm the transition found in [1], we find several new results that are unique to pseudo-gap systems.

We now give a summary of the results of the numerical RG calculations and their physical interpretation using an analysis that parallels Nozieres' Fermi liquid analysis of the ordinary Kondo fixed point. The technical details of the fixed-point analysis and a detailed description of the susceptibility are given below.

We start with the Hamiltonian given below that describes a spin- $\frac{1}{2}$ impurity, S , interacting antiferromagnetically at the origin with the local spin density of electrons which have a symmetric density of states $\rho(\epsilon) = [(1+r)/2]|\epsilon|^r$ with a band cut-off at $D_0 = 1$:

$$\begin{aligned} H_K &= \int_{-1}^1 \epsilon C_{\epsilon\sigma}^+ C_{\epsilon\sigma} \rho(\epsilon) d\epsilon - J_0 S \cdot \int_{-1}^1 \int_{-1}^1 C_{\epsilon\mu}^+ \frac{1}{2} \sigma_{\mu\nu} C_{\epsilon'\nu} \rho(\epsilon) \rho(\epsilon') d\epsilon d\epsilon' \\ &= \int_{-1}^1 \epsilon C_{\epsilon\sigma}^+ C_{\epsilon\sigma} \rho(\epsilon) d\epsilon - J_0 S \cdot f_{0\mu}^+ \frac{1}{2} \sigma_{\mu\nu} f_{0\nu} \end{aligned} \quad (1)$$

where

$$f_{0\mu} = \int_{-1}^1 \rho(\epsilon) C_{\epsilon\mu} d\epsilon$$

and a sum over the repeated spin index is assumed.

For $J < J_c$ the low-temperature behaviour is governed by an effective $J = -\infty$ fixed point where the localized electronic degree of freedom f_0 and the impurity spin are frozen out. For $r < 1/2$, calculations described in detail below lead to the following results for the temperature dependence of the effective moment $T\chi_{imp}$ at low temperatures (χ_{imp} is the impurity susceptibility defined as the total susceptibility minus the susceptibility of the pure system [2, 3]):

$$T\chi_{imp} = r/8 + \chi_1(T/T_K)^{1-r} + \chi_2(T/T_K)^{1-2r} \quad (2)$$

where χ_1 and χ_2 are constants (for $r = 0$ it can be shown that $\chi_1 = \chi_2$). In addition, the free energy is given by

$$F = -T(2r \ln 2 + F_1(T/T_K)^{1-r}). \quad (3)$$

Therefore, we have for the the entropy

$$S_{imp} = 2r \ln 2 + (2-r)F_1(T/T_K)^{1-r} \quad (4)$$

and the specific heat

$$C_{imp} = (2-r)(1-r)F_1(T/T_K)^{1-r}. \quad (5)$$

The constants χ_1 , χ_2 and F_1 are of the order of unity. It is worth noting that in the absence of the impurity spin the specific heat of the electrons at low temperatures is proportional to T^{1+r} and the susceptibility vanishes as T^r (or H^r as a function of the field); these results are a consequence of the pseudo-gap spectrum and reduce to well known results as $r \rightarrow 0$.

The crucial feature of the zero-temperature properties of the model is that both the effective moment $T\chi_{imp}$ and the entropy are non-zero. To understand these unusual properties better, we consider the following analysis, in the spirit of Nozieres' Fermi liquid description of the ordinary Kondo effect [6] which exploited a phase-shift analysis. At zero temperature, the impurity spin and f_0 electron form a singlet leading to a ground state which is a linear combination of the states with $f_{0\mu}^+ f_{0\mu} = 1$. If the up-spin conduction electron channel is constrained by the condition $f_0^+ f_0 = 1$, then the down-spin channel is constrained

by the condition $f_0^+ f_0 = 0$, and vice versa. The ground state can thus be characterized by studying the energy spectrum of the single-particle Hamiltonian (for a single channel)

$$H_p = \int_{-1}^1 \epsilon C_\epsilon^+ C_\epsilon \rho(\epsilon) d\epsilon + G f_0^+ f_0 \quad (6)$$

in the limit $G \rightarrow \pm\infty$. The term $G f_0^+ f_0$ represents potential scattering: the energy structure with the constraint $f_0^+ f_0 = 0$ or 1 is obtained by setting $G \rightarrow \infty$ or $-\infty$. To obtain the extra magnetic moment and entropy induced by this potential scattering, we first calculate the phase shift, and obtain from it the effective density of states, from which the zero-temperature physical properties can be evaluated. The phase shift $\delta^0(\epsilon)$ can be obtained using the relation

$$\tan \delta^0 = \lim_{G \rightarrow \pm\infty} \frac{\pi \rho(\epsilon)}{F(\epsilon) - 1/G} \quad (7)$$

where

$$\rho(\epsilon) = \frac{1+r}{2} |\epsilon|^r \quad F(\epsilon) = \int_{-1}^1 \frac{\rho(\epsilon') d\epsilon'}{\epsilon - \epsilon'} = \pi \rho(\epsilon) \tan\left(\frac{\pi r}{2}\right) \text{sgn}(\epsilon).$$

Thus we have the phase shift given by $\delta^0(\epsilon) = \pi/2 + (\pi r/2) \text{sgn}(\epsilon) + O(\epsilon^{1-r})$ irrespective of the sign of G (both channels of up-spin and down-spin electrons are described by the same phase shift). Using this phase shift, the change in the density of states can be evaluated: $\delta\rho(\epsilon) = (1/\pi) d\delta^0/d\epsilon = r \delta(\epsilon)$. It is this delta-function density of states that gives rise to the extra susceptibility and entropy:

$$\delta\chi = \frac{1}{2} \int_{-1}^1 \delta\rho'(\epsilon) f(\epsilon) d\epsilon = -\frac{r}{2} f'(0) = \frac{r}{8T} \quad (8)$$

or $T \delta\chi = r/8$. In the preceding equation $f(\epsilon) = 1/(1 + e^{\beta\epsilon})$ is the Fermi function. The extra entropy is given by

$$\delta S = 2 \int_{-1}^1 \delta\rho(\epsilon) \ln(1 + e^{-\beta\epsilon}) d\epsilon = 2r \ln 2. \quad (9)$$

These results confirm our fixed-point analysis. The delta function in the extra density of states reflects the difference between the pseudo-gap power-law density of states of the original electrons and the densities of states that are non-zero at the Fermi level. Such a difference can also give rise to qualitatively different results in other related problems. The Anderson orthogonality catastrophe is not operative and the overlap between Fermi seas with and without potential scattering is non-vanishing. This in turn leads to an additional delta-function contribution at the threshold for the XPS spectrum calculated with this power-law density of states. We have verified these results explicitly.

Wilson's RG method is a very powerful tool for studying magnetic impurities in metals that starts from a tridiagonalized Hamiltonian in which different energy scales are well separated. It is impossible to describe the method here and for details the reader is referred to [2, 3]. Previously the method was restricted to impurity problems with constant conduction electron densities of states due to the difficulty in obtaining the tridiagonalized Hamiltonian in the case of non-constant density of states. This difficulty has been overcome with a new tridiagonalization technique recently proposed by us [5]; this makes our current study possible.

The Hamiltonian in equation (1) can be discretized logarithmically (with the scaling factor Λ) and tridiagonalized using the procedure in [5]. The resulting tridiagonalized Hamiltonian can be written as

$$H_K = \frac{1 + \Lambda^{-1}}{2} \sum_{n=0}^{\infty} [\xi_n (f_{n\mu}^+ f_{n+1\mu} + \text{HC})] - J_0 S \cdot f_{0\mu}^+ \frac{1}{2} \sigma_{\mu\nu} f_{0\nu} \tag{10}$$

in terms of the Wilson basis set $\{f_n, n = 0, 1, \dots\}$ that consists of a hierarchy of states from the most localized high-energy state directly coupled to the impurity, f_0 , to spatially extended low-energy states. The coefficients $\{\xi_n\}$ are determined from the tridiagonalization procedure. To a very good accuracy we found that, for large n , $\xi_{n-1}/\xi_n = \Lambda^{1/2}$ when n is odd, and $\xi_{n-1}/\xi_n = \Lambda^{(1-r)/(2(1+r))}$ when n is even. This has been checked extensively for $r \leq 1$, numerically. When $r = 0$, which corresponds to the constant density of states, this result reduces to the analytical values for $\{\xi_n\}$ [2]. (Note that there is a difference of a factor of $\Lambda^{-n/2}$ between our definition of ξ_n and those in [2, 3].)

In order to carry out the RG calculation, we need to rescale the Hamiltonian at each iteration step. The rescaling is done by defining H_N as follows:

$$H_N = \frac{1}{\xi_{N-1}} \left\{ \sum_{n=0}^{N-1} [\xi_n (f_{n\mu}^+ f_{n+1\mu} + \text{HC})] - \frac{2}{1 + \Lambda^{-1}} J_0 S \cdot f_{0\mu}^+ \frac{1}{2} \sigma_{\mu\nu} f_{0\nu} \right\}. \tag{11}$$

The rescaling factor is $S_N = 2((1 + \Lambda^{-1})\xi_{N-1})$, which is proportional to $\Lambda^{N/(2(1+r))}$ for large N . The recursion relation that is the basis of our numerical RG calculation can now be written as

$$H_{N+1} = \frac{\xi_{N-1}}{\xi_N} H_N + (f_{N\mu}^+ f_{N+1\mu} + \text{HC}). \tag{12}$$

As we increase N , the system evolves from high temperatures to low temperatures. At a given N , the thermodynamic quantities are calculated for $T_N = 1/(\beta S_N)$ for a selected value of β . By studying the evolution of the many-body energy level structures we can obtain information near the fixed points of the Hamiltonian.

We now provide some of the technical details of the fixed-point analysis that underlie the results described earlier. We will analyse the fixed points of the Hamiltonian for various r and initial coupling J_0 . We follow [2, 3] and consider the $J = 0$ and $J = -\infty$ fixed points. The fixed-point Hamiltonian for the $J = 0$ fixed point is

$$H_N = \frac{1}{\xi_{N-1}} \sum_{n=0}^{N-1} [\xi_n (f_{n\nu}^+ f_{n+1\nu} + \text{HC})]. \tag{13}$$

There are two fixed points: one for even and another for odd N , just as in the case of the constant density of states. When N is odd, the single-particle energy levels (the example given here is for $r = 0.2$ and $\Lambda = 2.5$) are

$$\eta_j^* = \pm 0.73539, \pm 2.1339, \pm 4.6050, \dots, \pm \Lambda^{(j-1)(1+r)}, \dots, \tag{14}$$

while for even N , the single-particle energy levels are

$$\hat{\eta}_j^* = 0, \pm 1.4931, \pm 3.3920, \pm 7.2812, \dots, \pm \Lambda^{(j-1)(1+r)+1/2}, \dots. \tag{15}$$

We have also checked that f_0, f_2, f_4, \dots scale as $\Lambda^{-N/4}$, while f_1, f_3, f_5, \dots scale as $\Lambda^{-N(3+r)/(4(1+r))}$. Simple power counting reveals that there are no marginal and relevant operators around this fixed point. The three leading irrelevant operators are $o_1 \propto \Lambda^{N/(2(1+r))} S \cdot f_{0\mu}^+ \frac{1}{2} \sigma_{\mu\nu} f_{0\nu}$, $o_2 \propto \Lambda^{N/(2(1+r))} (f_{0\mu}^+ f_{1\mu} + \text{HC})$, and $o_3 \propto \Lambda^{N/(2(1+r))} (f_{0\mu}^+ f_{0\mu} - 1)^2$. o_1, o_2 , and o_3 scale with N as $\Lambda^{-Nr/(2(1+r))}$, $\Lambda^{-N/2}$, and $\Lambda^{-N(1+2r)/(2(1+r))}$ respectively.

Thus, for small values of the initial coupling J_0 , the $J = 0$ fixed point is stable. However, the fixed point is unstable for large coupling, as has been argued in [1]. By solving the perturbative scaling equation in [1], one can find a transition at $J_c = -2r/(1+r)$: for $J_0 < J_c$ the $J = 0$ fixed point is unstable. Numerical values of J_c are also very close to those obtained by perturbative scaling for small r . When the $J = 0$ fixed point becomes unstable the Hamiltonian evolves to a different fixed point at zero temperature. We find that for $r < 1/2$ this fixed point is the $J = -\infty$ fixed point described below; while for $r > 1/2$ the zero-temperature fixed point is a completely new one, the structure of which we still do not understand.

The Hamiltonian for the $J = -\infty$ fixed point (both the impurity spin operator and f_0 are frozen out) is

$$\bar{H}_N = \frac{1}{\xi_{N-1}} \sum_{n=1}^{N-1} [\xi_n (f_{n\mu}^+ f_{n+1\mu} + \text{HC})]. \quad (16)$$

Because ξ_{n-1}/ξ_n is not the same for even and odd n , the $J = -\infty$ fixed-point energy levels are not the same as those at the $J = 0$ fixed-point Hamiltonian. This is in contrast to the case of a constant density of states where the energy levels are the same except for an odd-even switch. When N is odd, the numerical results for the energy levels are:

$$\bar{\eta}_j^* = 0, \pm 1.2545, \pm 2.9109, \pm 6.2500, \dots, \pm \Lambda^{j/(1+r)-1/2}, \dots \quad (17)$$

while for an even N , the single-particle energy levels are

$$\hat{\eta}_j^* = \pm 0.63086, \pm 2.1247, \pm 4.6050, \dots, \pm \Lambda^{(j-1)/(1+r)}, \dots \quad (18)$$

In addition, we have also found that $f_1 \propto \Lambda^{-(1-r)N/(4(1+r))}$ and $f_2 \propto \Lambda^{-(3-r)N/(4(1+r))}$. As in the case of constant density of states, we can write down two leading irrelevant operators: $O_1 = w_1 \Lambda^{N/(2(1+r))} (f_{1\mu}^+ f_{2\mu} + \text{HC})$ and $O_2 = w_2 \Lambda^{N/(2(1+r))} (f_{1\mu}^+ f_{1\mu} - 1)^2$. It is easy to see that O_1 and O_2 scale as $\Lambda^{-N(1-r)/(2(1+r))}$ and $\Lambda^{-N(1-2r)/(2(1+r))}$ respectively.

For $r > 0$ O_2 is more dominant than O_1 . In fact, it becomes a relevant operator when $r > 1/2$. Thus, as we mentioned earlier, zero-temperature fixed point for $r > 1/2$, is different from the $J = -\infty$ fixed point. Returning to the case of $r < 1/2$, we have checked that the energy level structure at low temperatures is well described by adding these two operators to the fixed-point Hamiltonian. The magnitudes of w_1 and w_2 can be determined by fitting the energy levels. Since the irrelevant terms are of order 1 when $T = T_K$, w_1 and w_2 are of the order $(1/T_K)^{1-r}$ and $(1/T_K)^{1-2r}$ respectively.

With this fixed-point, single-particle, Hamiltonian we can calculate $T\chi_{imp}$ at $T = 0$. For odd N (the same result is obtained for the even- N fixed-point Hamiltonian) $T\chi(0)$ can be calculated using the formulas in [2, 3]:

$$T\chi(0) = \lim_{\beta \rightarrow 0, \Lambda \rightarrow 1} \left[\frac{1}{8} + \sum_{l=1}^{\infty} \frac{e^{-\beta \bar{\eta}_l^*}}{(1 + e^{-\beta \bar{\eta}_l^*})^2} - \sum_{l=1}^{\infty} \frac{e^{-\beta \hat{\eta}_l^*}}{(1 + e^{-\beta \hat{\eta}_l^*})^2} \right]. \quad (19)$$

The summations in the above formulas can be calculated using the trick explained in [2]; the result is $T\chi_{imp}(0) = r/8$. Similarly we can calculate the zero-temperature effective entropy for the impurity: $S_{imp}(0) = 2r \ln 2$. These results were given earlier. We can then calculate the contribution from O_1 and O_2 , following [3], without obtaining the explicit values for the coefficients, and these lead to the $(T/T_K)^{1-r}$ and $(T/T_K)^{1-2r}$ dependences shown in equations (2)–(5).

When $r > 1/2$, as we mentioned earlier, the ground state for $J_0 < J_c$ cannot be described by the $J = -\infty$ fixed point, which is essentially a pseudo-gap Fermi liquid with

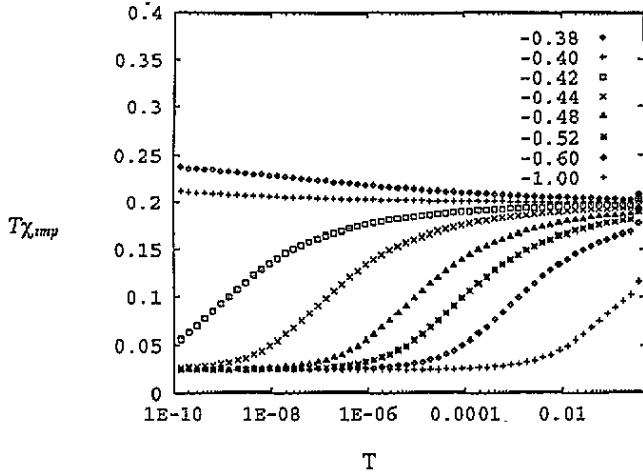


Figure 1. $T\chi_{imp}$ plotted as a function of T for $r = 0.2$ and $J_0 = -0.38, -0.40, -0.42, -0.44, -0.48, -0.52, -0.60$ and -1.0 . Note that there is a transition at around $J_0 \approx -0.40$ where the Kondo effect starts to show. Also note the non-zero magnetic moment when $T \rightarrow 0$.

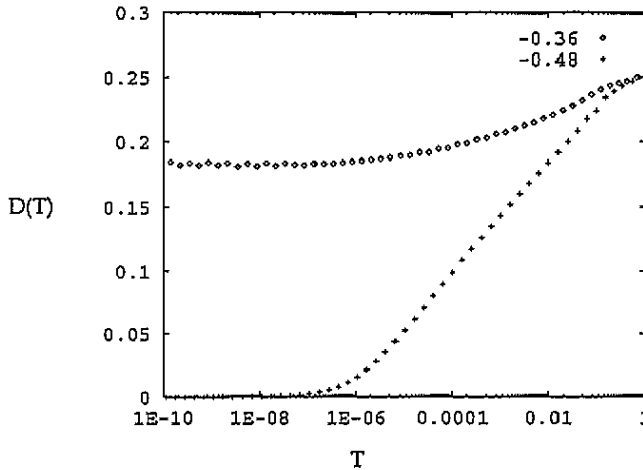


Figure 2. $D(T)$ plotted as a function of T for $r = 0.2$ and $J_0 = -0.36$ and -0.48 .

the density of states containing a delta-function component. We suspect that the ground state in this case may exhibit essentially non-Fermi liquid behaviour.

We now present our numerical results for the calculation of the impurity susceptibility χ_{imp} and zero-frequency response function $\langle\langle S_z; S_z \rangle\rangle$ (S_z is the z -component of the impurity spin), using the procedures explained in [2, 3] and [4] respectively.

Most of our calculations are done for $r = 0.05, 0.1, 0.2, 0.3, 0.4$ and 0.6 . $\Lambda = 2.5$ is used for the calculation of χ_{imp} and $\Lambda = 3.0$ is used for the calculation of $\langle\langle S_z; S_z \rangle\rangle$, except for the cases in which $r = 0.4$ and 0.6 where $\Lambda = 3.0$ and 4.0 are used respectively.

We first present our results for $r < \frac{1}{2}$. Figure 1 shows the temperature dependence of the susceptibility for the case $r = 0.2$ and selected values of J_0 . It is clear that there is a critical coupling J_c , separating the regime with the Kondo effect and the one without the Kondo effect. Also note the existence of a residual moment in the Kondo regime ($J_0 < J_c$). Figure 2 shows the zero-frequency response function $D(T) = T\langle\langle S_z; S_z \rangle\rangle$ in these two

regimes. In the case of constant density of states, $D(T)$ and $T\chi$ have the same temperature dependence, and for small J_0 their values are almost the same [4]. This is apparently not true with the power-law density of states. In particular $D(T)$ tends to zero as $T \rightarrow 0$; this suggests that the impurity spin itself is quenched, but there is a residual moment due to the contribution from conduction electron susceptibility.

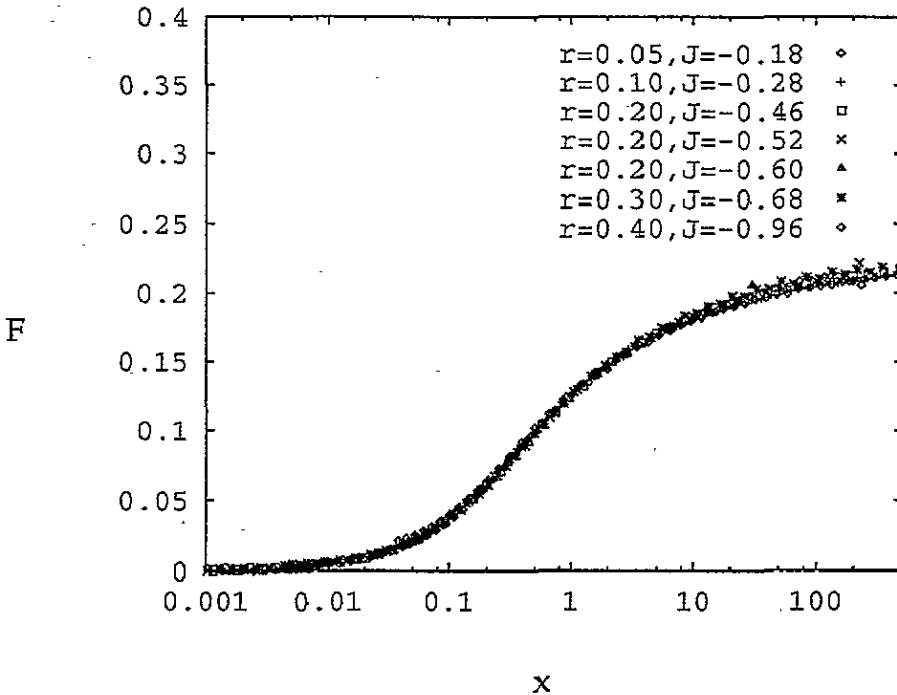


Figure 3. $F = (T\chi_{imp}(T) - r/8)/(1 - r - 3r^2/2)$ versus $x = \frac{1}{2}((T/T_K)^{1-2r} + (T/T_K)^{1-r})$ using the susceptibility data for $r = 0.05, 0.1, 0.2, 0.3,$ and 0.4 and selected values of J_0 , which are shown in the legend of the plot. The solid line represents the universal curve $f(x)$.

One of the important features of the Kondo problem is that thermodynamic quantities follow universal curves. To investigate universality in the case of the power-law density of states, we attempt to fit the impurity susceptibility using the function

$$T\chi_{imp}(T) = \frac{r}{8} + Bf(c_1(T/T_K)^{1-2r} + c_2(T/T_K)^{1-r}) \quad (20)$$

where T_K is the Kondo temperature and $f(x)$ is the universal function describing the susceptibility in the Kondo problem for a constant density of states. The form of the universal function is chosen by taking into account the fact that the leading low-temperature behaviour is given by equation (2). For $r = 0$ c_1 and c_2 are equal (since $\chi_1 = \chi_2$ in equation (2)); while for $r > 0$ c_1 and c_2 can be made equal by redefining T_K . We can thus set $c_1 = c_2 = 1/2$ in equation (20). The coefficient B is related to m_0 , the value of $T\chi_{imp}$ in the limit $T_K \ll T \ll D_0$: $B = 4(m_0 - r/8)$. Unfortunately, we do not have an analytical result for m_0 ; we have to choose B empirically. Our choice is $B = 1 - r - 3r^2/2$. From figure 3, it is clear that the data plot of $F = (T\chi_{imp}(T) - r/8)/B$ versus $\frac{1}{2}((T/T_K)^{1-2r} + (T/T_K)^{1-r})$ falls on the universal curve $f(x)$; this provides strong numerical evidence of universality. Note that when plotting the figure, T_K is chosen such that $F(T = T_K) = F_0$ with $F_0 = 0.125$.

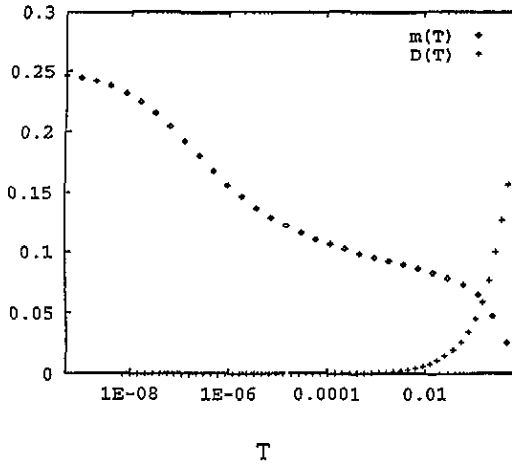


Figure 4. $T\chi_{imp}$, denoted as $m(T)$ in the legend, and $D(T)$ plotted as a function of T for $r = 0.6$ and $J_0 = -2.0$.

We have also investigated the dependence of the Kondo temperature as a function of J_0 for a given r . We find a linear relationship between T_K^r and versus J_0 , thus confirming the result obtained in [1]: $T_K \propto |J_0 - J_c|^{1/r}$.

We have also calculated $T\chi_{imp}(T)$ and $D(T)$ for the case $r > 1/2$. For $J_0 > J_c$ the impurity spin is not frozen as $T \rightarrow 0$, and there is no qualitative difference from the case $r < 1/2$. For $J_0 < J_c$ (the results are plotted in figure 4), on the other hand, there is qualitative difference, as expected from discussion previous. The impurity spin is quenched ($D(T) \rightarrow 0$ as $T \rightarrow 0$); however, there is no Kondo effect quenching in $T\chi_{imp}(T)$.

In conclusion we have performed a Wilson renormalization group calculation of the Kondo model with the density of states $\rho(\epsilon) = C|\epsilon|^r$, representing a pseudo-gap spectrum. A rich spectrum of interesting behaviours is found, some of which can be understood clearly in the framework of Wilson's RG calculation and associated fixed-point analysis: for weak coupling $J_0 > J_c \approx -2r$, there is no Kondo effect, and the system is shown to evolve to the $J = 0$ fixed point. On the other hand, for strong coupling $J_0 < J_c$, the system behaves quite differently for r less than or larger than $1/2$. For $r < 1/2$, the system is found to evolve to the $J = -\infty$ fixed point, and the susceptibility is found to fit the universal curve: $T\chi_{imp}(T) = r/8 + (1 - r - 3r^2/2)f(\frac{1}{2}((T/T_K)^{1-2r} + (T/T_K)^{1-r}))$. We have also argued that the ground state is effectively a pseudo-gap Fermi liquid with a delta-function excitation at the Fermi level. The delta-function component in the excitation spectrum gives rise to a residual moment and residual entropy. For $r > 1/2$, the $J = -\infty$ fixed point becomes unstable and the simple Fermi liquid picture breaks down. Although there is a quenching of the impurity spin, the total magnetic susceptibility does not show the Kondo effect.

References

- [1] Withoff D and Fradkin E 1990 *Phys. Rev. Lett.* **64** 1835
- [2] Wilson K G 1975 *Rev. Mod. Phys.* **47** 773
- [3] Krishnamurthy H R, Wilkins J W and Wilson K G 1980 *Phys. Rev. B* **21** 1003
- [4] Chen K, Jayaprakash C and Krishnamurthy H R 1992 *Phys. Rev. B* **15** 5368
- [5] Chen K and Jayaprakash C 1995 *Phys. Rev. B* at press
- [6] Nozieres P 1974 *J. Low Temp. Phys.* **17** 31